20th Australian International Aerospace Congress

ISBN number: 978-1-925627-66-4

Please select category below:

Normal Paper ☒
Student Paper ☐
Young Engineer Paper ☐

Bearing-Fault Signature Generation for Equipment Health Monitoring using a seven Degree-of-Freedom Bearing-Vibration-Model under non-steady Conditions

Philipp Schildt[1,2,3], Pier Marzocca[2], Carsten Braun[3], Wim Verhagen[2]

[1] *Rolls-Royce Electrical, Günther-Scharowsky-Str. 1, 91508 Erlangen, Germany, philipp.schildt@rolls-royce-electrical.com*

[2] *Royal Melbourne Institute of Technology, PO Box 71 Bundoora VIC 3083, Australia*

[3] *FH Aachen University of Applied Sciences, Hohenstaufenallee 6, 52064 Aachen, Germany*

Abstract

The advent of electric propulsion in aviation comes with the opportunity to further increase propulsion system safety and reduce maintenance efforts as systems are becoming mechanically less complex. In modern electrical machines, the remaining components subject to mechanical wear are basically the rotor-bearings. Optimized designs use the same bearing for the rotor of the electrical machine and the propeller. One key technology to reduce maintenance cost and increase safety is to detect upcoming faults in a very early stage to enable condition-based maintenance and calculate remaining useful life (RUL). Whilst conventional and artificial neural network (ANN)-based monitoring techniques are well proven against available bearing-fault-datasets in steady-conditions, bearing fault-detection and -classification becomes more complex in a non-steady environment. In this work, a 7- degree of freedom (DoF) bearing-fault model is used to synthesize high-resolution vibration data under different non-steady environments: Based on well validated 5-DoF simulation approaches, a bearing fault vibration model has been developed, allowing the synthesis of time-series signals for bearing-faults in a simulated (flight simulator) or recorded (flight experiments) environment. The model, implemented in MATLAB/Simulink, accounts for normal- and lateral-acceleration, pitch- and yaw-rates, propeller rotational-speed, and thrust-force to the bearing. By using simulated- and recorded-flight data, it can be shown that manoeuvring- and atmospheric-excitation has a significant impact on the bearing-fault vibration-signatures. The synthesized data can then be utilized to train ANN-based classifiers or regression-models, as well as to optimize detection algorithms based on conventional feature extraction for new propulsion-systems, before operational-data is available. Training and optimization of ANN-based classifiers is subject to ongoing work and not part of this paper.

Keywords: Equipment-Health-Monitoring, Electric-Propulsion, Advanced-Air-Mobility, Bearing-Fault-Diagnosis, Flight-Conditions, Remaining-Useful-Life, Distributed Propulsion.

Introduction

As the need for climate-neutral air transport evolves, electric propulsors as key enabler for battery-electric- or hybrid- flights become more and more important. Early Demonstrators, as the e-Genius [1] (maiden Flight in 2011) showed the general feasibility of battery-electric flight for longer distance travel with small aircraft. However mass constraints, especially with respect to the energy storage density of current battery technology, do not allow for longer commercial

missions, that are solely powered by batteries [2]. Besides operations with sustainable aviation fuel (SAF), hydrogen hybrid aircraft, like the APUS i-2 [3] are a very promising technology for lowest emission flights with renewable energy at reasonable range and cost. For higher power-classes, turbo-electric propulsion based on cryogenic hydrogen in combination with high-temperature-superconducting (HTS) electrical machines could be a key technology for mid- to long-range missions [4, 5]. In addition to hundreds of start-ups and several established aviation-companies that are thriving in the emerging eVTOL market with battery-electric concepts, in 2022 NEX launched the first hydrogen-powered long-range eVTOL [6].

In contrast to reciprocating aircraft engines, electric motors come along with significant lower inherent vibration and noise levels: Fig. 1 shows the vibration spectrum from 0 … 1200 Hz for a cruise segment from a Taifun 17E motorglider powered by a Limbach 2400 reciprocating engine (a) and the e-Genius motorglider powered by a Sineton 40 kW electric motor. Both aircraft are equipped with a 2-blade constant-speed propeller operating at 2400 RPM for the Taifun (a) and 1950 RPM for the eGenius (b). Signals were acquired with a Siemens SCADAS XS mobile data recorder and PCB / ICP shear-type accelerometers in aircraft z-direction, directly at the motor housing. *Note: Scale for graph b) y-axis is 10-times higher than for a).*

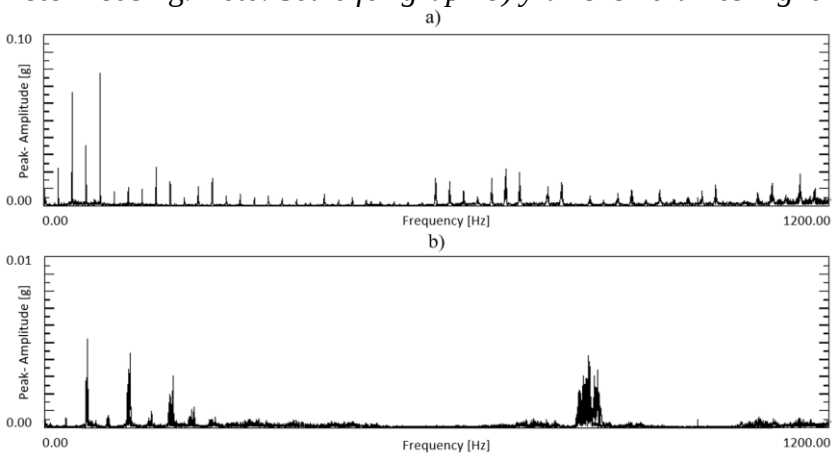

Fig. 1: Healthy Motor-Vibration Spectrum
(a): Limbach 2400 - reciprocating engine (Taifun 17E)
(b) Sineton 40 kW – electric motor (e-Genius)

These low-noise signals offer the opportunity, to detect bearing faults in an early stage, long before they become critical. Depending on the aircraft design and the criticality of the motor bearings, predictive maintenance approaches are enabled, allowing e.g. for opportunistic grouping of maintenance, as described in [7].

Methodology

Based on the work of [8], several simulation models for a deep grove ball bearing were developed [9–11].[12] used these simulations to drive machine-learning for bearing-fault classification. Based on the work of [11] the bearing fault model was further modified to 7-degrees of freedom (DoF), as illustrated in Fig. 2. This allows for signature generation in two dimensions (aircraft y- and z-axis), as well as for a varying contact angle and shaft-speed input, influencing the characteristic fault frequencies. This became necessary, as most of the available condition monitoring methods, fault datasets, and simulation-models are emphasizing stationary or quasi-stationary inertial- and operating-point conditions. However, during flight operations in general aviation, advanced air mobility or commuter-transport, flight-phases with quasi-stationary conditions are very few compared to long-haul operations, where besides gentle and infrequent maneuvers, also atmospheric disturbances are usually avoided by avoiding significant weather or simply flying above it during cruise.

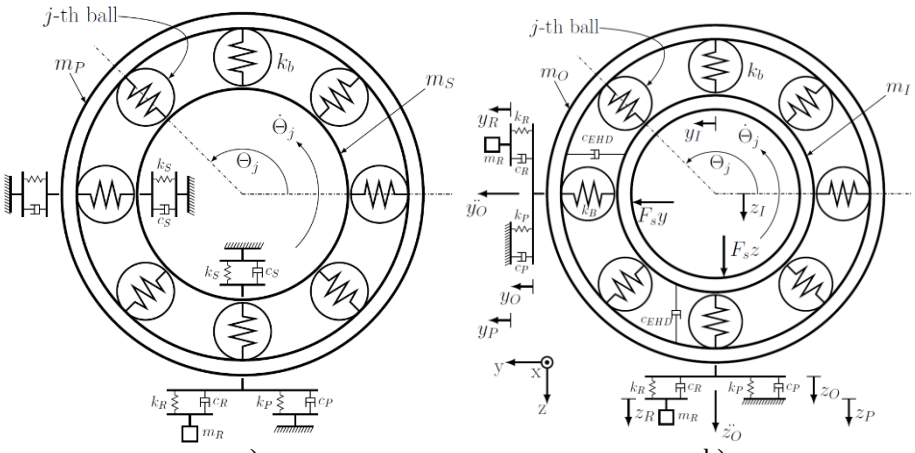

a) b)

Fig. 2: - 5 DoF Bearing Model from [11] (a) and derived 7-DoF Model

The model is implemented in MATLAB / Simulink ® and allows for the input of varying shaft-forces due to gyroscopic- and inertial-forces, which are calculated from either a flight-simulation input or recorded data from flight-experiments as illustrated in Fig. 3.

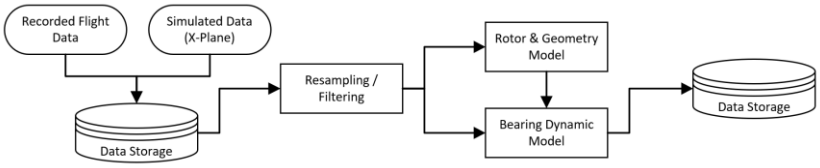

Fig. 3 - Data Flow Diagram

Simulated Flights

As a reference-input for signature generation, two simulated datasets are used. Both consist of a traffic pattern flown by a Cessna 172, as a typical representative of a 4-seater general aviation aircraft and are simulated in X-Plane. The simulation includes a constant-speed propeller model, as well as atmospheric turbulence and is based on blade-element-theory aircraft modelling [13], granting a realistic response to pilot-inputs and atmospheric excitation. An extract of the data input to the bearing-fault simulation is illustrated in Fig. 4 for a flight in calm air and a flight with simulated atmospheric turbulence. Additional inputs to the bearing-fault simulation are thrust, load-factors in y- and z-direction, as well as the propeller RPM.

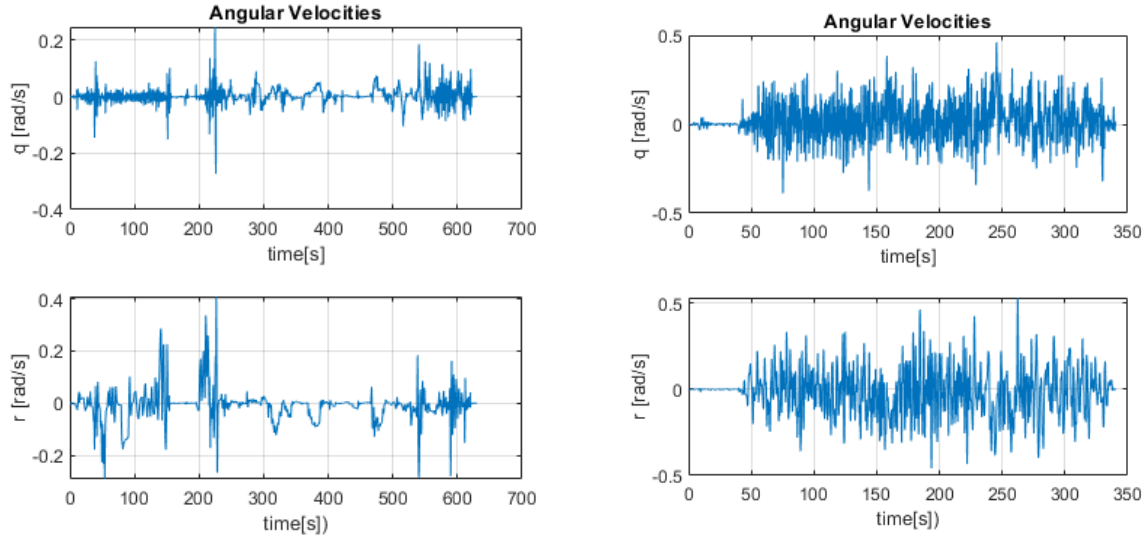

a) *b)*

Fig. 4: Cessna 172 Simulated Flights a): No Turbulence b) Turbulence

Recorded Flights

To further validate the simulated data and to gather reliable real-world data, flights with the Stemme S10VTX airborne research platform from FH Aachen University were conducted under several atmospheric conditions [14]. The data from the high-frequency accelerometers and the lower-frequency inertial-navigation-system data are combined with a Kalman-Filter and fed into the 7-DoF Bearing Fault Model, as illustrated in Fig. 5.

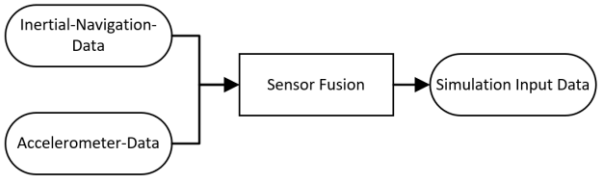

Fig. 5: Fusion of Accelerometer and INS Data

Fig. 6 shows the recorded accelerations after the sensor fusion and the angular velocities from Flight ID14 from [14]. Different to the two simulated flights, this flight was in thermal conditions, and the aircraft was circling in several thermals, having a visible effect on the normal acceleration n_z as well as on the heading-rate q.

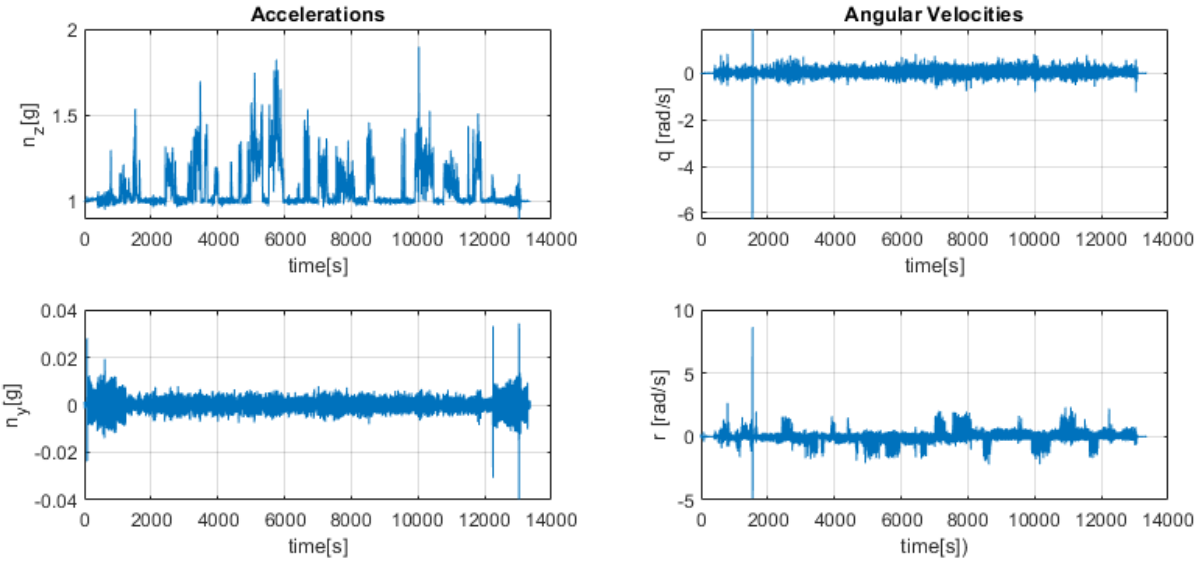

Fig. 6: Recorded Flight Data [14]

Results

A Total of 625 simulations with different damage-sizes, damage positions, and input-inertial data has been performed. Some of the results are shown here. Fig. 7 gives a comparison of a spectrum for an outer-race fault simulated with the 5-DoF Model from [11] and the modified 7-DoF-model.

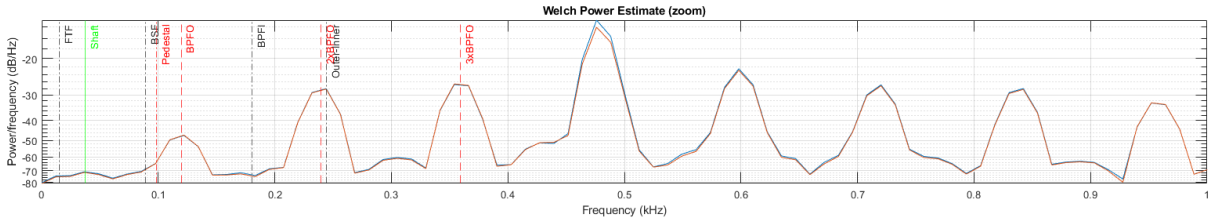

Fig. 7: Power-Spectrum of z-axis vibration of a bearing-fault in steady-state (blue: 5-DoF Model [11], orange: 7-DoF Model)

Additionally, the some relevant eigenmodes and the characteristic bearing frequencies (BPFO: Ball-Pass-Frequency Outer-Race, BPFI: Ball-Pass-Frequency Inner-Race, FTF: Fundamental Train Frequency, and BSF: Ball-Spin-Frequency) are marked as dotted lines. A good correlation between both models can be observed.

Bearing Loads

The load direction and RMS Value of the drive-end (DE) bearing was calculated for two simulated and one recorded flight. The distribution of the load direction is illustrated in Fig. 8 for the 3 cases as logarithmic polar histograms.

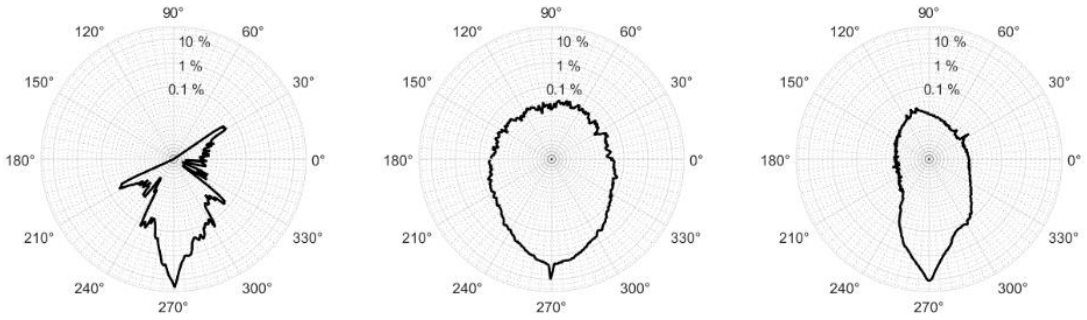

a) b) c)

Fig. 8: Bearing-Load Direction for different Flights: No Turbulence, Simulated (a) and Turbulent Flight, Simulated (b), and Recorded Stemme Flight (c)

All three distributions have a prominent peak at 270°, accounting for the gravity-loading of the bearing in steady states. Whilst the bearing-load-angle for simulated turbulent flight (b) and the Stemme flight (c) are smoothly distributed, the calm-air flight (a) is more discrete as an artifact of the different manoeuvring phases. Fig. 8 shows exemplarily a time series and belonging power-spectrum, with a medium size bearing fault at the outer race in position 270°.

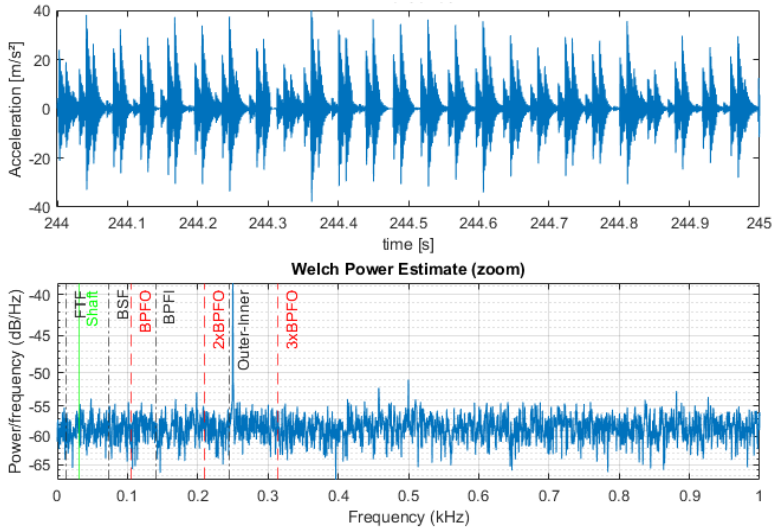

Fig. 8: Exemplary Time-Series for outer-race fault, simulated with a recorded flight data

Compared to the clear steady-state spectrum (Fig. 7), a significant increase of noise is visible and the combined outer-inner eigenfrequency becomes predominant. Overall, the comparison of simulated data with recorded flight data from Stemme S10VTX shows, that when taking atmospheric turbulence into the model, the load-distributions and the resulting bearing fault signatures become similar.

Concluding Remarks and Outlook

A solution for bearing fault signature generation in a flight environment using X-Plane and MATLAB / Simulink was presented. As maneuvering- and atmospheric induced loads have a significant effect on the fault-signatures of a single bearing defect, using a flight-simulation is an efficient approach to generate realistic training-data for the use in machine-learning based condition monitoring, that can easily be adopted to other aircraft-types or configurations. Future work of the authors is focusing on the optimization of ANN-based RUL estimation for electric propulsion under flight conditions.

Acknowledgments

I gratefully express appreciation for my colleagues at Siemens and Rolls-Royce, as well as FH Aachen University and RMIT University for supporting this work in several manners.

Data Availability

The Matlab / SIMULINK code used for the data generation, as well as examples of the generated data, are online available at github: https://github.com/phschildt/7DoF_Bearing_Fault

References

[1] L. Schumann, "*Reduktion des Energiebedarfs mittels eines batterieelektrischen Antriebs am Beispiel eines Kleinflugzeugs*," Dissertation, Institut für Flugzeugbau, Universität Stuttgart, Stuttgart, 2018. Accessed: Nov. 6 2022. [Online]. Available: https://elib.uni-stuttgart.de/bitstream/11682/9767/3/Diss_Len_Schumann.pdf

[2] M. Hepperle, "Electric Flight - Potential and Limitations.," in *AVT-209 Workshop on ENERGY EFFICIENT TECHNOLOGIES AND CONCEPTS OPERATION*.

[3] APUS Group, *APUS i-2: The Zero Emission GA Aircraft.* [Online]. Available: https://apus-zero.de/wp-content/uploads/2021/09/APUS_i-2_20210901.pdf (accessed: Nov. 6 2022).

[4] M. Filipenko, S. Biser, M. Boll, M. Corduan, M. Noe, and P. Rostek, "Comparative Analysis and Optimization of Technical and Weight Parameters of Turbo-Electric Propulsion Systems," *Aerospace*, vol. 7, no. 8, p. 107, 2020, doi: 10.3390/aerospace7080107.

[5] M. Corduan, M. Boll, R. Bause, M. Oomen, M. Filipenko, and M. Noe, "Topology comparison of superconducting AC machines for hybrid-electric aircraft," *IEEE Trans. Appl. Supercond.*, vol. 30, no. 2, pp. 1–10, 2020, doi: 10.1109/TASC.2019.2963396.

[6] W. Tacke, "E-surprises in Berlin: More e-Exhibitions in Germany," *eFlight Journal*, no. 3, pp. 16–20, 2022.

[7] Juseong Lee, Ingeborg de Pater, Stan Boekweit, Mihaela Mitici, "Remaining-Useful-Life prognostics for opportunistic grouping of maintenance of landing gear brakes for a fleet of aircraft," in *Proceedings of the 7th European Conference of the Prognostics and Health Management Society 2022, Turin, Italy, July 6th-July 8th, 2022.* [Online]. Available: https://phm-europe.org/wp-content/uploads/2022/06/ProPHME22.pdf

[8] N. S. FENG, E. J. HAHN, and R. B. Randall, "USING TRANSIENT ANALYSIS SOFTWARE TO SIMULATE VIBRATION SIGNALS DUE TO ROLLING ELEMENT BEARING DEFECTS," in *Applied mechanics: Progress and applications ; proceedings of the Third Australasian Congress on Applied Mechanics, Sydney, Australia, 20 - 22 February 2002*, Sydney, Australia, 2002, pp. 689–694.

[9] N. Sawalhi and R. B. Randall, "Simulating gear and bearing interactions in the presence of faults," *Mechanical Systems and Signal Processing*, vol. 22, no. 8, pp. 1924–1951, 2008, doi: 10.1016/j.ymssp.2007.12.001.

[10] S. Sassi, B. Badri, and M. Thomas, "A Numerical Model to Predict Damaged Bearing Vibrations," *Journal of Vibration and Control*, vol. 13, no. 11, pp. 1603–1628, 2007, doi: 10.1177/1077546307080040.

[11] C. Mishra, A. K. Samantaray, and G. Chakraborty, "Ball bearing defect models: A study of simulated and experimental fault signatures," *Journal of Sound and Vibration*, vol. 400, pp. 86–112, 2017, doi: 10.1016/j.jsv.2017.04.010.

[12] C. Sobie, C. Freitas, and M. Nicolai, "Simulation-driven machine learning: Bearing fault classification," *Mechanical Systems and Signal Processing*, vol. 99, pp. 403–419, 2018, doi: 10.1016/j.ymssp.2017.06.025.

[13] X-Plane, *How X-Plane Works.* [Online]. Available: https://www.x-plane.com/desktop/how-x-plane-works/

[14] J. Keimer, *Flight Test for Determination of Atmospheric Turbulence Data for Application in A/C Condition Monitoring Systems*. Master-Thesis. Aachen, 2019.